Published by :
http://www.ijert.org

International Journal of Engineering Research & Technology (IJERT)
ISSN: 2278-0181
Vol. 10 Issue 03, March-2021

Mathematical Model and Sensitivity Analysis of a Parallel 3-Phase Voltage Source Inverter

Khalid Ateea Alfaitori
Benghazi University, Faculty of Information Technology
Benghazi, Libya

Haytham Yousef Mustfa
Electrical System Technology Department
College of Electrical and Electronics Technology-Benghazi

Saad. M. Saad
College of Electrical and Electronics Technology-Benghazi

Naser El Naily
College of Electrical and Electronics Technology-Benghazi

***Abstract*—Recently, there has been a great interest in grid connected renewable energy resources such as photovoltaic, fuel cells and wind energy. Typically, parallel-connected three phase voltage source inverters are utilized in these grid connected renewable energy applications. In this paper, modeling and control of a parallel three phase voltage source inverter is considered. To set the stage, the inverter model is derived by defining the variations in the output d-q voltages and d-q currents as the system states. The variation in duty cycle is defined as the control input. The system control is implemented using two different control strategies, i.e., (voltage control mode of the first inverter and power control mode of the second inverter). To optimize the system performance, the sensitivity analysis is applied to the inverter model. To verify the eigenvalue analysis, time-domain simulation is used to determine the effects of controller and parameter variations on the system stability.**

KeyWords:- Parallel inverter; sensitivity analysis; eigenvalue location; SVPWM

I. INTRODUCTION

The surge of applications of power electronics in industrial, commercial, military, aerospace, and residential areas has driven many research studies in this subject [1]. The objective of these studies is mainly to obtain, highly reliable and efficient power electronic components with low cost and compact size. In addition, power electronics play an important role in the advancement of distributed energy resources [1]. Due to their environmental and economic benefits compared to large power plants, the reliance on distributed power sources, such as fuel cells, wind turbines and photovoltaic systems has increased in the recent years. However, these sources do not necessarily generate the desired rated voltage and frequency. Therefore, a voltage source inverter (VSI) is required to be used as an interface between the distributed energy source and the main grid as shown in Fig. 1. Distributed power sources in microgrid can operate in parallel to the grid or in the islanded mode [2]. Consequently, many research has focused recently on the use of a set of inverters connected in parallel.

Parallel connected inverters enable the load current to be shared among different distributed resources and the main grid. As a result, the reliability of the whole power generation system will be improved. Due to the existence of large number of power converters, the stability problem becomes increasingly important in distributed energy systems. To improve the stability and the performance of the distributed energy resource, small-signal modeling of the parallel voltage source inverter system is considered [2], [3].

There are many research papers provide an extended review for control techniques of parallel inverters, [4]-[6]. The control strategies may be classified as centralized and decentralized control strategies [4]. The centralized control strategy has many good advantages. For instance, the current sharing is forced at all times even during transient, and different power rating inverters can be connected without changing the control structure. The system may also be easily maintained and replaced. However, this strategy has a few serious disadvantages. One of the major disadvantages is due to the reference voltage and current signals that have to be sent to all inverters in the network. This requires a high bandwidth communication link in the system which is sensitive to nonlinear loads. On the other hand, Master/Slave control method gives a good load sharing and synchronization. The main disadvantage of the master/slave method is that it is not redundant since it has a single point of failure.

Furthermore, there are excellent features of the current/power sharing control technique; they have a load sharing with a very good transient response and less circulating current between the inverters. This technique has some problems such as, it is not easily expendable and it requires an interconnection which make the system less reliable. The distributed control strategy, on the other hand, is based on the rotational reference frame rather than stationary reference frame. A current sharing in the system is provided in steady state and during transient. Lower communication bandwidth is needed. However, this strategy is not appropriate for unbalanced systems. Droop control method has many desirable features such as expandability, modularity, redundancy, and flexibility. There are as well some drawbacks such as, slow transient response and possibility of circulating current. These reviews lead to the control techniques of parallel inverter which are classified according to mode of operation, and these techniques still require development to overcome some challenges. For instance, a sensitivity analysis should be carried out to achieve system stability.

In this paper, a general control system model with two different control modes of parallel operated inverters are discussed. The average model of the parallel operated voltage source inverters is based on a phase leg and small signal model.

International Journal of Engineering Research & Technology (IJERT)
ISSN: 2278-0181
Vol. 10 Issue 03, March-2021

Then the performance of parallel connected voltage source inverter with voltage control strategy of first inverter and power control strategy of second inverter and frequency domain analysis are validated by time-domain simulation.

The organization of this paper will be as follows: the full model of the two parallel-connected three phase voltage source inverters is derived in Section II. In Section III the control strategies and the closed loop system are considered. Section IV discusses the eigenvalue Loci and sensitivity analysis. Finally, the study presented in this paper is concluded in Section V.

II. MATHEMATICAL MODEL OF 3-PHASE VSIS CONNECTED IN PARALLEL

The average small-signal models of the parallel three-phase voltage source inverter are presented in this section. The switching network averaging is performed on a phase-leg basis. After the phase-leg averaging, the average model of a three-phase voltage source inverter may be easily established by connecting three averaged phase legs [1], [7].The typical circuit of two parallel three-phase voltage source inverters with different DC sources is shown in Fig. 1.

From the average model of parallel VSI the state-space equations can be derived and which will be as follows:

$$\frac{d}{dt}\begin{bmatrix} i_{a1} \\ i_{b1} \\ i_{c1} \end{bmatrix} = \frac{1}{L_1}\begin{bmatrix} d_{a1} \\ d_{b1} \\ d_{c1} \end{bmatrix} V_{dc1} - \frac{1}{L_1}\begin{bmatrix} V_{AN} \\ V_{BN} \\ V_{CN} \end{bmatrix} - \frac{1}{L_1}\begin{bmatrix} V_N \\ V_N \\ V_N \end{bmatrix} \quad (1)$$

$$\frac{d}{dt}\begin{bmatrix} i_{a2} \\ i_{b2} \\ i_{c2} \end{bmatrix} = \frac{1}{L_2}\begin{bmatrix} d_{a2} \\ d_{b2} \\ d_{c2} \end{bmatrix} V_{dc2} - \frac{1}{L_2}\begin{bmatrix} V_{AN} \\ V_{BN} \\ V_{CN} \end{bmatrix} - \frac{1}{L_2}\begin{bmatrix} V_N \\ V_N \\ V_N \end{bmatrix} \quad (2)$$

$$\frac{d}{dt}\begin{bmatrix} V_{AN} \\ V_{BN} \\ V_{CN} \end{bmatrix} = \frac{1}{2C}\begin{bmatrix} i_{a1} \\ i_{b1} \\ i_{c1} \end{bmatrix} + \frac{1}{2C}\begin{bmatrix} i_{a2} \\ i_{b2} \\ i_{c2} \end{bmatrix} - \frac{1}{RC}\begin{bmatrix} V_{AN} \\ V_{BN} \\ V_{CN} \end{bmatrix} \quad (3)$$

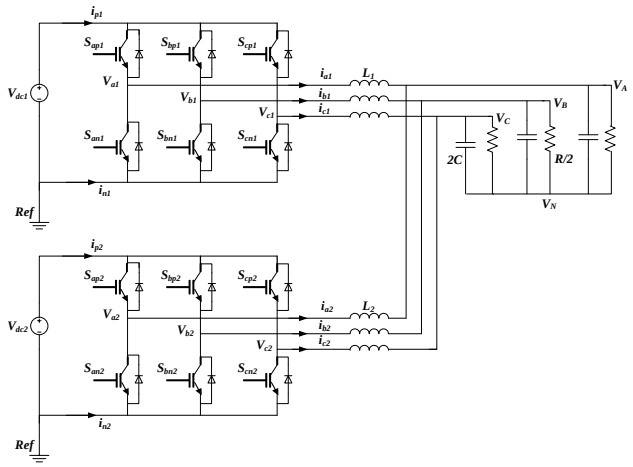

Fig. 1: Circuit schematic of parallel three-phase inverters

To linearize the system to design controllers, the model in the stationary coordinates is usually transformed into rotating coordinates. Then, one can obtain the average model of the parallel voltage source inverters in the rotating coordinates:

$$\frac{d}{dt}\begin{bmatrix} i_{d1} \\ i_{q1} \\ i_{z1} \end{bmatrix} = \frac{1}{L_1}\begin{bmatrix} d_{q1} \\ d_{d1} \\ d_{z1} \end{bmatrix} V_{dc1} - \frac{1}{L_1}\begin{bmatrix} V_d \\ V_q \\ V_z \end{bmatrix} - \frac{1}{L_1}\begin{bmatrix} 0 \\ 0 \\ 3V_N \end{bmatrix} - \begin{bmatrix} 0 & -\omega & 0 \\ \omega & 0 & 0 \\ 0 & 0 & 0 \end{bmatrix}.\begin{bmatrix} i_{d1} \\ i_{q1} \\ i_{z1} \end{bmatrix} \quad (4)$$

$$\frac{d}{dt}\begin{bmatrix} i_{d2} \\ i_{q2} \\ i_{z2} \end{bmatrix} = \frac{1}{L_2}\begin{bmatrix} d_{q2} \\ d_{d2} \\ d_{z2} \end{bmatrix} V_{dc2} - \frac{1}{L_2}\begin{bmatrix} V_d \\ V_q \\ V_z \end{bmatrix} - \frac{1}{L_2}\begin{bmatrix} 0 \\ 0 \\ 3V_N \end{bmatrix} - \begin{bmatrix} 0 & -\omega & 0 \\ \omega & 0 & 0 \\ 0 & 0 & 0 \end{bmatrix}.\begin{bmatrix} i_{d2} \\ i_{q2} \\ i_{z2} \end{bmatrix} \quad (5)$$

$$\frac{d}{dt}\begin{bmatrix} v_d \\ v_q \\ v_z \end{bmatrix} = \frac{1}{2C}\begin{bmatrix} i_{d1} \\ i_{q1} \\ i_{z1} \end{bmatrix} + \frac{1}{2C}\begin{bmatrix} i_{d2} \\ i_{q2} \\ i_{z2} \end{bmatrix} - \frac{1}{RC}\begin{bmatrix} v_d \\ v_q \\ v_z \end{bmatrix} - \begin{bmatrix} 0 & -\omega & 0 \\ \omega & 0 & 0 \\ 0 & 0 & 0 \end{bmatrix}.\begin{bmatrix} v_d \\ v_q \\ v_z \end{bmatrix} \quad (6)$$

The model can be simplified based on $i_z = i_{z1} = -i_{z2} \approx 0$. The linearization of the large-signal time average model around the operating point is based on assuming that the input DC power sources are ideal, thus,

$$\frac{d}{dt}\begin{bmatrix} \tilde{i}_{d1} \\ \tilde{i}_{q1} \end{bmatrix} = \frac{1}{L_1}\begin{bmatrix} \tilde{d}_{d1} \\ \tilde{d}_{q1} \end{bmatrix} V_{dc1} - \frac{1}{L_1}\begin{bmatrix} \tilde{v}_d \\ \tilde{v}_q \end{bmatrix} - \begin{bmatrix} 0 & -\omega \\ \omega & 0 \end{bmatrix}.\begin{bmatrix} \tilde{i}_{d1} \\ \tilde{i}_{q1} \end{bmatrix} \quad (7)$$

$$\frac{d}{dt}\begin{bmatrix} \tilde{i}_{d2} \\ \tilde{i}_{q2} \end{bmatrix} = \frac{1}{L_2}\begin{bmatrix} \tilde{d}_{d2} \\ \tilde{d}_{q2} \end{bmatrix} V_{dc2} - \frac{1}{L_2}\begin{bmatrix} \tilde{v}_d \\ \tilde{v}_q \end{bmatrix} - \begin{bmatrix} 0 & -\omega \\ \omega & 0 \end{bmatrix}.\begin{bmatrix} \tilde{i}_{d2} \\ \tilde{i}_{q2} \end{bmatrix} \quad (8)$$

$$\frac{d}{dt}\begin{bmatrix} \tilde{v}_d \\ \tilde{v}_q \end{bmatrix} = \frac{1}{2C}\left(\begin{bmatrix} \tilde{i}_{d1} \\ \tilde{i}_{q1} \end{bmatrix} + \begin{bmatrix} \tilde{i}_{d2} \\ \tilde{i}_{q2} \end{bmatrix}\right) - \begin{bmatrix} \frac{1}{RC} & -\omega \\ \omega & \frac{1}{RC} \end{bmatrix}.\begin{bmatrix} \tilde{v}_d \\ \tilde{v}_q \end{bmatrix} \quad (9)$$

Now, the state space equation of the small-signal model of parallel voltage source inverters May be achieved. The state variables are defined as $[\tilde{v}_d \tilde{v}_q \tilde{\imath}_{d1} \tilde{\imath}_{q1} \tilde{\imath}_{d2}\, \tilde{\imath}_{q2}]^T$ and the output variables are $[\tilde{d}_{d1} \tilde{d}_{q1} \tilde{d}_{d2} \tilde{d}_{q2}]^T$ which represent the control variables.

$$\dot{\tilde{x}} = A\tilde{x} + B\tilde{u} \quad (10)$$

$$\tilde{y} = C\tilde{x} \quad (11)$$

where, $\tilde{x}$ is the state variables' matrix and $\tilde{y}$ is the output matrix then:

$$\tilde{x} = [\tilde{v}_d \tilde{v}_q \tilde{\imath}_{d1} \tilde{\imath}_{q1} \tilde{\imath}_{d2}\, \tilde{\imath}_{q2}]^T \quad (12)$$

$$\tilde{u} = [\tilde{d}_{d1} \tilde{d}_{q1} \tilde{d}_{d2} \tilde{d}_{q2}]^T \quad (13)$$

$$C = I \quad (14)$$

Therefore, the state space equations can be obtained and the state and input matrices may be respectively expressed as:

$$A = \begin{bmatrix} \frac{-1}{RC} & \omega & \frac{1}{2C} & 0 & \frac{1}{2C} & 0 \\ -\omega & \frac{-1}{RC} & 0 & \frac{1}{2C} & 0 & \frac{1}{2C} \\ \frac{-1}{L_1} & 0 & 0 & \omega & 0 & 0 \\ 0 & \frac{-1}{L_1} & -\omega & 0 & 0 & 0 \\ \frac{-1}{L_2} & 0 & 0 & 0 & 0 & \omega \\ 0 & \frac{-1}{L_2} & 0 & 0 & -\omega & 0 \end{bmatrix} \quad (15)$$

$$B = \begin{bmatrix} 0 & 0 & 0 & 0 \\ 0 & 0 & 0 & 0 \\ \frac{V_{dc1}}{L_1} & 0 & 0 & 0 \\ 0 & \frac{V_{dc1}}{L_1} & 0 & 0 \\ 0 & 0 & \frac{V_{dc2}}{L_2} & 0 \\ 0 & 0 & 0 & \frac{V_{dc2}}{L_2} \end{bmatrix} \quad (16)$$

III. CONTROL STRATEGY AND CLOSED LOOP SYSTEM

The control scheme of each inverter consists of two cascaded control loops. The inner control loops independently regulate the inverter output current in the rotating reference frame, i_d and i_q. The outer loops in the voltage control mode are used to produce the d-q axis current references for the inner loops by regulating the voltage at given reference values. In power control mode, the outer loops are used to regulate the active and

International Journal of Engineering Research & Technology (IJERT)
ISSN: 2278-0181
Vol. 10 Issue 03, March-2021

reactive power at a given operating point and provide the current references, $i_{d\text{-}ref}$ and $i_{q\text{-}ref}$, in the rotating reference frame for the inner loops [8], [9].

Voltage control mode is used for the first inverter is depicted in Fig.2. The instantaneous values of the first inverter's output current components in rotating reference frame $i_{d1\text{-}ref}$ and $i_{q1\text{-}ref}$ are used to control the output voltage.

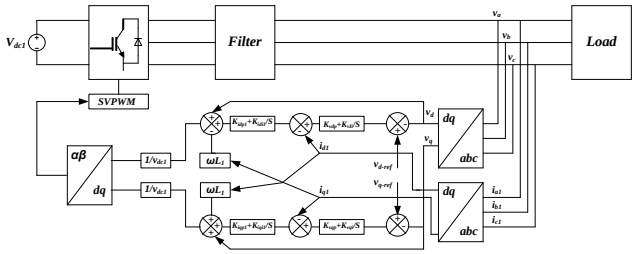

Fig. 2: First inverter with voltage control mode

The voltage at given references in voltage control mode is regulated by the outer loops to produce the d-q axis current references for the inner loops [8]. Therefore, the output of the outer voltage controller is inputted to the inner control loop and thus a proportional-integral (P-I) controller is used. Then:

$$\tilde{\imath}_{d1-ref} = \left(K_{vdp} + \frac{K_{vdi}}{s}\right)\left(\tilde{v}_{d-ref} - \tilde{v}_d\right) \quad (17)$$

$$\tilde{\imath}_{q1-ref} = \left(K_{vqp} + \frac{K_{vqi}}{s}\right)\left(\tilde{v}_{q-ref} - \tilde{v}_q\right) \quad (18)$$

In order to generate the gate control signals that drive the switches of the inverter, the outputs from this inner current loops are inputted to the Space Victor Pulse Width Modulation (SVPWM) module [8], [9], [10]. The duty cycles signals are given as:

$$\tilde{d}_{d1}.V_{dc1} = \left(K_{idp1} + \frac{K_{idi1}}{s}\right)\left(\tilde{\imath}_{d1-ref} - \tilde{\imath}_{d1}\right) - \omega L_1\tilde{\imath}_{q1} + \tilde{v}_d \quad (19)$$

$$\tilde{d}_{q1}.V_{dc1} = \left(K_{iqp1} + \frac{K_{iqi1}}{s}\right)\left(\tilde{\imath}_{q1-ref} - \tilde{\imath}_{q1}\right) + \omega L_1\tilde{\imath}_{d1} + \tilde{v}_q \quad (20)$$

The second inverter is using power control mode. The instantaneous values of the second inverter's output current components $i_{d2\text{-}ref}$ and $i_{q2\text{-}ref}$ are used to control the output active and reactive power respectively as shown in Fig 3.

In the power control mode, the active and reactive power are controlled at given set points by the outer loops to produce the d-q axis current references for inner loops [8]. Where:

$$P = \frac{3}{2}\left(V_d i_{d2} + V_d i_{q2}\right) \quad (21)$$

$$Q = \frac{3}{2}\left(V_q i_{d2} - V_d i_{q2}\right) \quad (22)$$

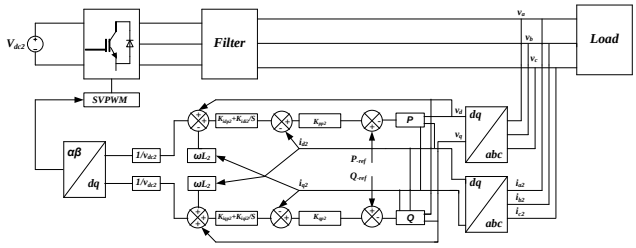

Fig. 3: Second inverter with power control mode

The outputs of these outer controllers are the inputs to the inner control loops. A proportional (P) controller is adopted. Thus,

$$\tilde{\imath}_{d2-ref} = \left(K_{Pp2}\right)\left(P_{ref} - P_2\right) \quad (23)$$

$$\tilde{\imath}_{q2-ref} = \left(K_{Qp2}\right)\left(Q_{ref} - Q_2\right) \quad (24)$$

The duty cycle signals of the second inverter may be given as:

$$\tilde{d}_{d2}.V_{dc2} = \left(K_{idp2} + \frac{K_{idi2}}{s}\right)\left(\tilde{\imath}_{d2-ref} - \tilde{\imath}_{d2}\right) - \omega L_2\tilde{\imath}_{q2} + \tilde{v}_d \quad (25)$$

$$\tilde{d}_{q2}.V_{dc2} = \left(K_{iqp2} + \frac{K_{iqi2}}{s}\right)\left(\tilde{\imath}_{q2-ref} - \tilde{\imath}_{q2}\right) + \omega L_2\tilde{\imath}_{d2} + \tilde{v}_q \quad (26)$$

The dynamic behavior of the two parallel-connected inverters including their controllers may be investigated by using a linearized small- signal model of the control loops [7], [9]. Then, according the small- signal model of the control loops, the duty cycles of the two inverters operated in parallel with different DC power sources may be written as:

$$\tilde{d}_{d1} = \frac{1}{V_{dc1}}\left[\left(1 - K_{idp1}K_{vdp}\right)\tilde{v}_d - K_{idp1}\tilde{\imath}_{d1} - \omega L_1\tilde{\imath}_{q1} + K_{idp1}K_{vdi}\tilde{\emptyset}_{d1} + K_{idi1}\tilde{\gamma}_{d1} + K_{idp1}K_{vdp}\tilde{v}_{d-ref}\right] \quad (27)$$

$$\tilde{d}_{q1} = \frac{1}{V_{dc1}}\left[\left(1 - K_{iqp1}K_{vqp}\right)\tilde{v}_q + \omega L_1 i_{d1} - K_{iqp1}i_{q1} + K_{iqp1}K_{vqi}\tilde{\emptyset}_{q1} + K_{iqi1}\tilde{\gamma}_{q1} + K_{iqp1}K_{vqp}\tilde{v}_{q-ref}\right] \quad (28)$$

$$\tilde{d}_{d2} = \frac{1}{V_{dc2}}\left[\left(1 - \frac{3}{2}K_{idp2}K_{pp2}I_{d2}\right)\tilde{v}_d - \frac{3}{2}K_{idp2}K_{pp2}I_{q2}\tilde{v}_q - \left(\frac{3}{2}K_{idp2}K_{pp2}V_d + K_{idp2}\right)\tilde{\imath}_{d2} - \left(\frac{3}{2}K_{idp2}K_{pp2}V_q + \omega L_2\right)\tilde{\imath}_{q2} + K_{idi2}\tilde{\gamma}_{d2} + K_{idp2}K_{pp2}\tilde{P}_{ref}\right] \quad (29)$$

$$\tilde{d}_{q2} = \frac{1}{V_{dc2}}\left[\frac{3}{2}K_{iqp2}K_{Qp2}I_{q2}\tilde{v}_d + \left(1 - \frac{3}{2}K_{iqp2}K_{Qp2}I_{d2}\right)\tilde{v}_q + \left(\omega L_2 - \frac{3}{2}K_{iqp2}K_{Qp2}V_q\right)\tilde{\imath}_{d2} + \left(\frac{3}{2}K_{iqp2}K_{Qp2}V_d - K_{iqp2}\right)\tilde{\imath}_{q2} + K_{iqi2}\tilde{\gamma}_{q2} + K_{iqp2}K_{Qp2}\tilde{\emptyset}_{ref}\right] \quad (30)$$

The small signal model of controller provides six new state variables, which are: ($\tilde{\emptyset}_{d1}$ $\tilde{\emptyset}_{q1}$ $\tilde{\gamma}_{d1}$ $\tilde{\gamma}_{q1}$ $\tilde{\gamma}_{d2}$ $\tilde{\gamma}_{q2}$).

Therefore, the control output can be expressed as:

$$\tilde{u} = H_1[\tilde{z}] + J\left[\left(\tilde{v}_d\tilde{v}_q\tilde{P}\tilde{Q}\right)_{ref}\right] \quad (31)$$

The complete model of the closed loop system may be expressed as:

$$\frac{d}{dt}[\tilde{z}] = (A_1 + B_1H_1)[\tilde{z}] + B_2\left[\left(\tilde{v}_d\tilde{v}_q\tilde{P}\tilde{Q}\right)_{ref}\right] \quad (32)$$

where

$$z = [\tilde{v}_d\tilde{v}_q\tilde{\imath}_{d1}\tilde{\imath}_{q1}\tilde{\imath}_{d2}\tilde{\imath}_{q2}\tilde{\emptyset}_{d1}\tilde{\emptyset}_{q1}\tilde{\gamma}_{d1}\tilde{\gamma}_{q1}\tilde{\gamma}_{d2}\tilde{\gamma}_{q2}]^T \quad (33)$$

The order of the overall closed loop system is the twelfths, because there are 12 state variables (N=12). In frequency domain, we can get:

$$\frac{z(s)}{R(s)} = (SI - A_1 - B_1H_1)^{-1}.B_2 \quad (34)$$

where: $R(s) = [(\tilde{v}_d\tilde{v}_q\tilde{P}\tilde{Q})_{ref}](S)$, A_1 and B_1 are the state and the input matrices of the closed loop system.

IV. EIGENVALUE LOCI AND SENSITIVITY ANALYSIS

The locations of eigenvalues move with controller and system parameters in the frequency domain. The movement of eigenvalues by these parameters leads to unsatisfactory oscillatory response. Various loci of closed loop poles by changing a controller and system parameters are presented in

International Journal of Engineering Research & Technology (IJERT)
ISSN: 2278-0181
Vol. 10 Issue 03, March-2021

this section in order to further study the level of eigenvalue sensitivity. All eigenvalues of the system are given in Table I.

TABLE I
THE EIGENVALUES OF PARALLEL INVERTERS SYSTEM

Eigenvalues	
$-3.189*10^{5}$	$-1.2745*10^{5}$
$-1.0695*10^{4} \pm 3.14*10^{-3}i$	$-125 \pm 9.682*10^{-4}i$
$-50 \pm 1.118*10^{-3}i$	-150.177
$-4.110*10^{-7} \pm 1.21*10^{-8}i$	-100.031

Two real eigenvalues are very close to the origin point are influenced by increasing K_{vdi} from 0 to 4000 as shown in Fig. 4. When K_{vdi} is increasing from 0 to 400,one of these real eigenvalues at the origin point and another is very close to the origin point move toward each other and become a pair of complex conjugate poles near to origin point. This results in improvement of damping ratio and increase in system stability.

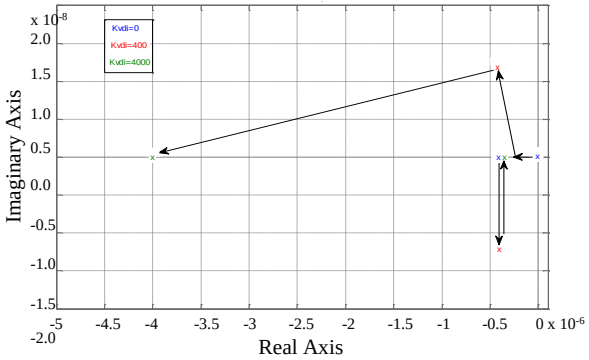

Fig. 4:The eigenvalues location with an increasing K_{vdi}

Then K_{vdi} is more than 400, these complex eigenvalues become two real poles which are less influenced by Kvdi. Therefore, K_{vdi} is selected to be 400 or any value more than 400.

In Fig. 5, K_{vqi} is increasing from 0 to 4000, while all other parameters are set to be constant. There are two real eigenvalues influenced by K_{vqi}. When K_{vqi} is increasing from 0 to 400 one real pole at origin point moves towards the other real pole that is very close to the origin point and become a pair of complex conjugate poles with more stable because improvement of damping ratio. This pair of complex conjugate eigenvalues with K_{vqi} more than 400 becomes two real eigenvalues with less sensitivity to the variation of K_{vqi}. So K_{vqi} is set to be 400 or any other value more than 400.

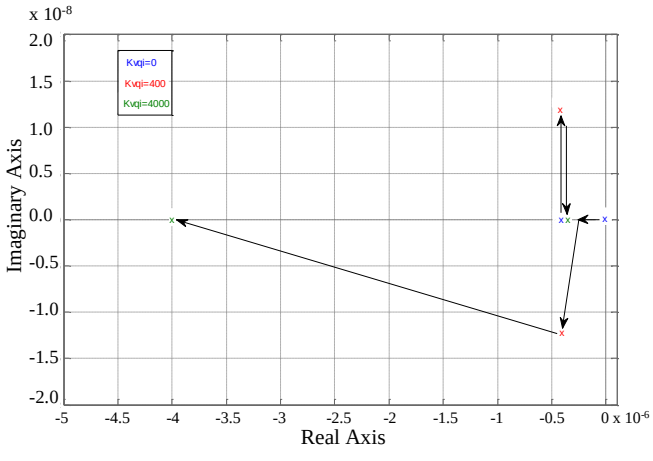

Fig. 5:The eigenvalues location with an increasing K_{vqi}

The loci of the eigenvalues which influenced by current controller parameters of first inverter K_{idp1} in the frequency domain are shown in Fig. 6.

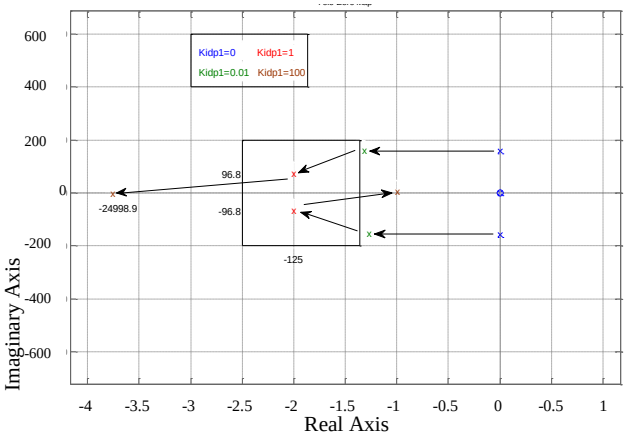

Fig. 6:The eigenvalues location with an increasing K_{idp1}

When K_{idp1} equals zero, the system is unstable because there are a pair of complex conjugate poles in the right half plane. When it is increased to about 0.01, these eigenvalues move from the right half plan (RHP) to the left half plan (LHP) and continue to move away from the origin point until K_{idp1} equals 1. With K_{idp2} increasing from 0 to 0.01, a pair of complex conjugate eigenvalues moves from RHP to the LHP, thereby the system moves to stable state as shown in Fig. 7. When $K_{idp2}$is increased from 0.01 to 1, this pair of complex conjugate eigenvalues becomes a pair of two real eigenvalues with less overshoot and oscillations.

Furthermore, when $K_{idp2}$is increased from 1 to 100, one of these real eigenvalues moves quickly towards origin point which reduce the system stability, and another real eigenvalue moves far away from origin point towards LHP. This shows the stability of the system is less sensitive to this eigenvalue. So K_{idp2} is set to be 1.

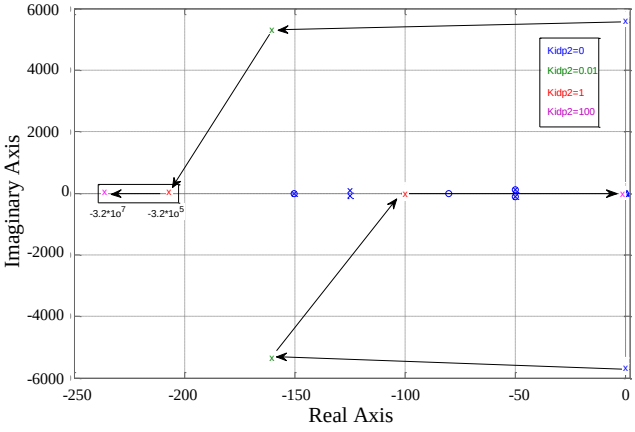

Fig. 7:The eigenvalues location with an increasing K_{idp2}

Fig. 8 shows the loci of eigenvalues which are influenced by filter parameter L. When L is increasing from 4 mH to 100 mH there are two a pair of complex conjugate eigenvalues moves quickly towards origin point and two real poles move toward

International Journal of Engineering Research & Technology (IJERT)
ISSN: 2278-0181
Vol. 10 Issue 03, March-2021

imaginary axis horizontally on the real axis. This leads to a decrease in system stability.

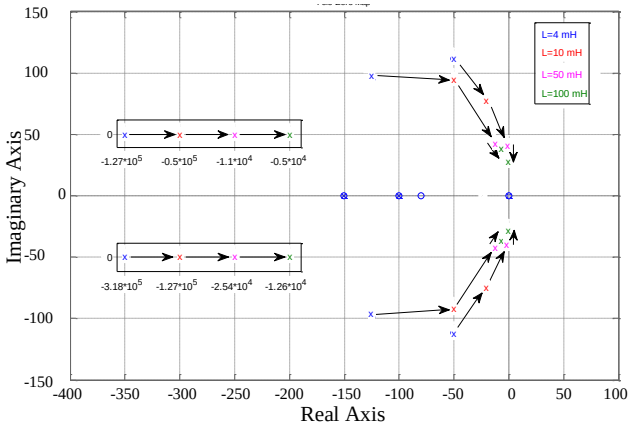

Fig. 8:The eigenvalues location with an increasing L

The reference value of the three phase output voltages peak is set to be 170V. Initially the active and reactive power of the second inverter are 10KW and 2KVAR respectively. These values are reduced by 50% after 0.35 seconds. The reference frequency is set to be 50 Hz. The simulation is run for 0.5 seconds and results under two different control strategies which are carried out and used to verify the eigenvalue analysis.

The time-domain simulation with L variation is shown in Fig. 9. When L is set as 4 mH the active power of the second inverter converges to high stable state with small oscillation compared to the two other values. From these simulation results, the system has large oscillation when this parameter is decreased to 0.63 mH. The stability of the system is reduced with high overshoot when L equals 10 mH. This is almost consistent with the frequency-domain analysis.

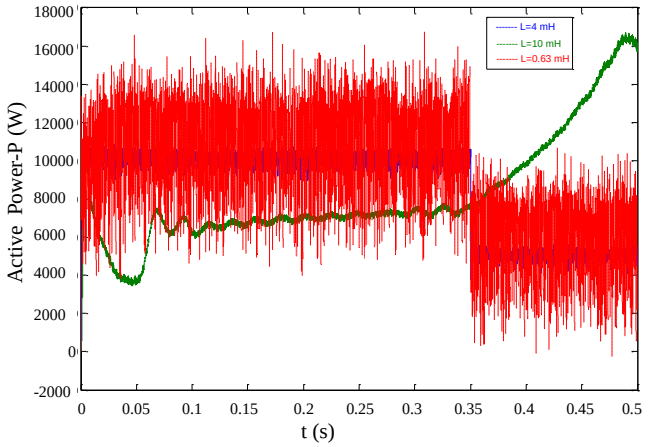

Fig. 9:Output active power of second inverter with an increasing L

V. CONCLUSION

In this paper, control strategies of two inverters operated in parallel were considered. The control strategy of the first inverter was based on the voltage control mode while the power control mode was used for the second inverter. Herein, two different DC sources were modeled based on an averaged model of the inverter. Using MATLAB/SIMULINK simulation, the performances of these strategies is evaluated. The eigenvalue analysis of the small-signal model which is based on the averaged model was also verified by the simulation results. The simulation results were also used to determine the effects of the controller and system parameter variations on the system stability. By recognizing the control and filter parameters that achieve the best response of the system, designers would be capable of improving the performance of the system.

REFERENCES

[1] Zhihong Ye, Modeling and Control of Parallel Three-Phase PWM Converters. Dissertation Submitted to the Faculty of the Virginia Polytechnic Institute and State University in Partial Fulfillment of the Requirements for the Degree of Doctor of Philosophy Electrical Engineering, September 15, 2000.

[2] Vandoorn, Tine, Bert Renders, Frederik De Belie, Bart Meersman, and Lieven Vandevelde. "A voltage-source inverter for microgrid applications with an inner current control loop and an outer voltage control loop." In International Conference on Renewable Energies, and Power Quality (ICREPQ09). 2009.

[3] Yu Zhang, Small-Signal Modeling and Analysis of Parallel- Connected Power Converter Systems for Distributed Energy Resources. Submitted to the Faculty of the University of Miami in Partial Fulfillment of the Requirements for the Degree of Doctor of Philosophy. May 2011.

[4] Prodanovic, M., Green, T.C., &Mansir, H. . "Survey of control methods for three-phase inverters in parallel connection". In the Proceedings of the 8th IEEE Conference on Power Electronics and Variable Speed Drives, 2000, pp.) 472-477.

[5] De Brabandere, Karel, Bruno Bolsens, Jeroen Van den Keybus, Achim Woyte, Johan Driesen, and Ronnie Belmans. "A voltage and frequency droop control method for parallel inverters." IEEE Transactions on power electronics 22, no. 4 (2007): 1107-1115.

[6] Mazumder, Sudip K., Muhammad Tahir, and Kaustuva Acharya. "Master–slave current-sharing control of a parallel DC–DC converter system over an RF communication interface." IEEE Transactions on Industrial Electronics 55, no. 1 (2008): 59-66.

[7] Coelho, Ernane Antonio Alves, Porfirio Cabaleiro Cortizo, and Pedro Francisco Donoso Garcia. "Small-signal stability for parallel-connected inverters in stand-

[8] Coelho, Ernane Antonio Alves, Porfirio Cabaleiro Cortizo, and Pedro Francisco Donoso Garcia. "Small-signal stability for parallel-connected inverters in stand-alone AC supply systems." *IEEE Transactions on Industry Applications* 38, no. 2 (2002): 533-542.

[9] Khalid Ateea Alfaitori, Ashraf Khalil, and Ali Asheibi. "Distributed Control of Photovoltaic-Based Microgrid."4th International Conference on Renewable Energy Research and Applications Palermo, Italy, 22-25 Nov 2015.

[10] Khalil, Ashraf, Khalid Ateea Alfaitori, and Ahmed Elbarsha. "Stability analysis of parallel-inverters in microgrid." In Automation and Computing (ICAC), 2014 20th International Conference on, pp. 110-115. IEEE, 2014.

[11] Yu Zhang, "Small-Signal Modeling and Analysis of Parallel- Connected Power Converter Systems for Distributed Energy Resources" PhD thesis, University of Miami, 2011.